International Journal of Pressure Vessels and Piping 208 (2024) 105120

Contents lists available at ScienceDirect

International Journal of Pressure Vessels and Piping

journal homepage: www.elsevier.com/locate/ijpvp

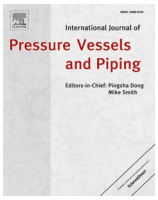

Modelling of hydrogen diffusion leading to embrittlement in austenitic stainless steels

P. Cavaliere *, B. Sadeghi, A. Perrone, D. Marsano, A. Marzanese

Department of Innovation Engineering, University of Salento, Via per Arnesano, 73100, Lecce, Italy

ARTICLE INFO

Keywords:
Hydrogen embrittlement
Traps
Microstructure
Finite element modelling
Diffusion

ABSTRACT

The paper presents the 3-D model of the hydrogen diffusion in austenitic stainless steel. In order to model the material behaviour, a real microstructure taking into account the grain boundaries, the dislocations density, the vacancies number and the precipitates state was analysed in order to the implemented in the employed software (ANSYS). The effect of each single hydrogen trap was physically determined. The simulations were carried out by modelling the material microstructure with a high number of elements and nodes in order to improve the affordability of the obtained results. The model allowed to identify the hydrogen diffusion mode in different conditions by evaluating the weight that each single trap has on the overall process. The developed model allowed also to define the hydrogen saturation of the microstructure in different conditions of temperature.

1. Introduction

1.1. Hydrogen embrittlement

The decrease in the metal's ductility generated by hydrogen absorption is known as hydrogen embrittlement (HE), it' also known as hydrogen-assisted cracking or hydrogen-induced cracking (HIC). Small hydrogen atoms have the capacity to penetrate solid metals. Hydrogen, once absorbed, reduces the force necessary for metal crack to begin and spread, leading to embrittlement [1,2]. Steels are particularly susceptible to hydrogen embrittlement, along with iron, nickel, titanium, cobalt, and their alloys [3,4].

Hydrogen embrittlement is dependent from temperature [5,6]. At temperatures above 150 °C, most metals are moderately resistant to hydrogen embrittlement [7]. Hydrogen embrittlement requires the existence of both atomic ("diffusible") hydrogen and a mechanical stress to cause fracture formation [8–10]. High strength materials are typically more brittle due to hydrogen embrittlement [11,12].

Two different types of hydrogen sources (gaseous hydrogen and hydrogen produced chemically at the metal surface) can expose metals to hydrogen. Gaseous hydrogen is molecular hydrogen, which does not produce embrittlement. Because atomic hydrogen readily dissolves into metal at ambient temperature, it is atomic hydrogen from chemical assault that causes embrittlement [13,14]. Pipelines and pressure vessels both contain gaseous hydrogen. Hydrogen can be produced electrochemically by acid, corrosion, and electroplating [15,16].

The phenomena of hydrogen embrittlement depend on how the atoms diffuse into the microstructure of the steel. Hydrogen is the smallest chemical element. It diffuses through metals more easily than any other element. When hydrogen atoms diffuse metals become brittle. Hydrogen diffuses by normal interstitial site diffusion or dislocation transport [17,18].

On the diffusion process, hydrogen trapping at defects has a significant impact. Dislocation, grain boundaries, precipitates and other defects are called traps. Because hydrogen diffuses so rapidly, even small traps can have a large impact on the diffusivity [19–21].

The model presented by McNabb and Foster [22] is the first model that regard the mobility of dissolved hydrogen in an iron lattice containing trapping sites. A diffusion equation with terms for sources and sinks was introduced. Oriani [10] reformulated the model of McNabb and Foster by adopting the assumption of local equilibrium between the mobile and the trapped populations of hydrogen for a constrained region. Yazdipour et al. [23] studied the role of grain boundaries for hydrogen diffusion in X70 steel. The conducted simulations revealed a faster diffusion of hydrogen atoms in larger grains compared to smaller ones, aligning well with the results of permeation tests. Additionally, the researchers noted the migration of hydrogen atoms across grain boundaries, where they gathered until reaching a critical concentration. Subsequently, diffusion occurred within the grains. Tekkaya et al. [24] conducted a simulation study on modeling of local hydrogen

* Corresponding author.
E-mail address: pasquale.cavaliere@unisalento.it (P. Cavaliere).

https://doi.org/10.1016/j.ijpvp.2023.105120
Received 11 April 2023; Received in revised form 13 December 2023; Accepted 25 December 2023
Available online 10 January 2024

Table 1
Hydrogen diffusion parameters for micro alloy steels.

Temperature [°C]	$D_{H_0}\left[\frac{mm^2}{s}\right]$	Q $\left[\frac{kJ}{mol}\right]$
$\alpha - range\ (0-740)$	1.07 E−01	11.14
$\gamma - range(740-1400)$	2.84 E−01	31.59
$\delta - range(1400-1540)$	17.05 E−01	42.71
liquid state (> 1540)	8.49 E−01	31.57

concentration on microscopic scale to characterize the influence of stress states and non-metallic inclusions in pipeline steels. Their results demonstrated that the impurity degree of the steel in terms of non-metallic inclusions plays an important role in hydrogen susceptibility in two aspects, namely geometrically (notch-effect) and in the generation of residual stresses. The effect of matrix shrinkage on the inclusions and the resulting stress field after cooling leads to the accumulation of hydrogen atoms around the inclusions, resulting in locally high critical concentrations. They also reported that local peak of the hydrogen concentration in the microstructure depends on the stress state. Maximum local hydrogen concentration is observed under biaxial tension, while the minimum concentration is obtained under uniaxial tension. the difference between maximum and minimum concentration is around 11 %. Sesen et al. [25] using DFT and MD analyses showed that the first entering hydrogen atoms are trapped at phase boundaries, increasing the ferrite phase's hardness but reducing the austenite phase's hardness. However, once the boundaries are passivated by hydrogen (more hydrogen concentration than before), further entering hydrogen can diffuse rapidly without energy barriers, resulting in softening of both phases. Tao et al. [26] used 2d RVEs meshed with quadratic elements and implemented hydrogen diffusion model under considering different diffusivity as well as solubility values for corresponding phases to model hydrogen diffusion in ferrite and austenite by the case of a duplex stainless steel. They concluded that hydrogen diffusion mainly takes place in ferrite and stretched austenite grains lead to higher diffusivity. Yang et al. [27] established a two-dimensional calculation model to simulate the formation of CPFs at the crack tip and its effects on the crack tip stress status and hydrogen diffusion. The results indicate that the corrosion product films can inhibit the hydrogen permeation into the crack tip, and the hydrostatic pressure effects on the redistribution of the permeated hydrogen are significant under larger external load conditions.

1.2. Hydrogen diffusion and trapping models

The process through which matter is introduced into a material because of molecular motions is called diffusion. Normal interstitial lattice sites or atomic and microstructural defects like vacancies, grain boundaries, voids, dislocations, cracks, etc. may be occupied by hydrogen during diffusion [28]. Traps are the names given to these latter defects. Atomic hydrogen can recombine to form hydrogen gas in voids or cracks [29,30]. These kinds of traps may hold a theoretically indefinite number of hydrogen atoms. There is a limit to how many hydrogen atoms can fit into traps like dislocations and grain boundaries, for this reason they are called saturable traps [31,32]. Considering a defect-free microstructure, hydrogen diffuses by moving along interstitial sites, due to its small size. The principle of the lattice diffusion consists in series of jumps from one site to another interstitial site. This jump requires sufficient activation energy E_a to overcome the energetic barrier. Using C_L as the hydrogen concentration in lattice site, one may estimate the hydrogen volume concentrations at typical interstitial lattice sites. It is typically assumed that hydrogen atoms diffuse through the crystal lattice according to Fick's law (eq. (1)).

$$\overline{J} = -D_L * \nabla C_L \tag{1}$$

Where J is the hydrogen flux vector, D_L is the hydrogen lattice diffusion coefficient. The hydrogen diffusion coefficient is function of temperature, position, and time, but they can be calculated according to an Arrhenius-like relationship (eq. (2)).

$$D_L = D_{L_0} * \exp\left(-\frac{E_a}{RT}\right) \tag{2}$$

where D_{L_0} is the pre-exponential factor, R is the universal gas constant, T is the absolute temperature, and E_a is the activation energy to move between two adjacent lattice sites. The trends of the flux and concentration lead to the definition of the hydrogen diffusion parameters relating to the Arrhenius relationship as reported in Table 1.

If the material is subject to stress, the hydrostatic stress gradient, σ_H, helps the diffusion of hydrogen towards regions with a higher value of σ_H. In this case the hydrogen flux vector expression (eq. (3)) becomes [33]:

$$\overline{J} = -D_L * \nabla C_L + \frac{D_L V_H C_L}{RT} \nabla \sigma_H \tag{3}$$

where V_H is the partial molar volume of hydrogen. In the diffusion processes, the number of hydrogen atoms is conserved. Because hydrogen concentration can change over time at any location in a transient diffusion process, Fick's first law must be changed in order to account for this variation in hydrogen flux. The gradient of hydrogen exiting at the exit surface after arriving at the entry surface can be simply expressed by eq. (4).

$$\frac{\partial \overline{J}}{\partial x} dx = J_{OUT} - J_{IN} \tag{4}$$

By assuming that the hydrogen diffusion coefficient is constant, the variation of the concentration over the time is expressed by eq. (5).

$$\frac{\partial C_L}{\partial t} = -\nabla * \overline{J} = D_L \nabla^2 C_L \tag{5}$$

In presence of mechanical stresses eq. (5) becomes (eq. (6)):

$$\frac{\partial C_L}{\partial t} = D_L \nabla^2 C_L + D_L \nabla * \left(\frac{V_H C_L}{RT} \nabla \sigma_H\right) \tag{6}$$

1.3. Hydrogen diffusion in lattice with traps

A site where the hydrogen chemical potential is lower than it is in an interstitial site is considered a trapping site from a thermodynamic approach. The many microstructural imperfections (vacancies, dislocations, etc.) act as hydrogen traps, raising the activation energy needed to break through the energetic barrier. Grain boundaries are the predominant defects that favourite the hydrogen transportation and consequent metals brittleness. Grain boundaries are believed to provide high diffusion paths for hydrogen, more particularly those with high misorientations. Research have discovered that the diffusion process is accelerated in boundary grains [34]. Grain boundary are the biggest volume traps in metal microstructures, for this reason his effects are the most relevant [35]. Vacancies interact strongly with interstitial hydrogen in most of metals [36]. Hydrogen easily fills the vacancies, the amount of hydrogen that can fill a vacancy is proportional to its size. The concentration of the vacancy is low at room temperature. The hydrogen trapping at vacancies may decrease hydrogen diffusion coefficients [37].

Dislocations are linear defects produced in metals by plastic deformation and grain growth processes. These defects cause distortions of the crystal lattice, these distortions cause that hydrostatic stresses are developed in proximity to the dislocation core [38]. Described by trapping models, dislocations generate several trap sites, with different trapping energies. Dislocation acts as a reversible trap in the edge and as an irreversible trap in the core [39].

Hydrogen uptake and hydrogen desorption behaviours show a dependence on the quantity and the size of precipitates. The amount of hydrogen that can be trapped in a precipitate is proportional to the size

of the precipitate.

1.4. Hydrogen trapping models

Most diffusion models based on hydrogen diffusion refer to the mathematical model of McNabb & Foster. Oriani reformulated the model using local equilibrium hypotheses.

It's important to modify the previous Fick's laws to considering the traps. C_T is the hydrogen volume concentration in trap sites. By considering C_T greater than zero, eq. (5) becomes eq. (7).

$$\frac{\partial(C_L + C_T)}{\partial t} = -\nabla J \tag{7}$$

If D_L is assumed constant in the material, eq. (7) can be modified as (eq. (8)):

$$\frac{\partial C_L}{\partial t} + \frac{\partial C_T}{\partial t} = D_L \nabla^2 C_L \tag{8}$$

In presence of mechanical stresses (eq. (9)):

$$\frac{\partial C_L}{\partial t} + \frac{\partial C_T}{\partial t} = D_L \nabla^2 C_L + D_L \nabla * \left(\frac{V_H C_L}{RT} \nabla \sigma_H \right) \tag{9}$$

The equation formulated by McNabb and Foster is the following (eq. (10)):

$$\frac{\partial \theta_T}{\partial t} = kC_L(1 - \theta_T) - p\theta_T \tag{10}$$

Where, θ_T is the fractional occupancy of traps, k and p are two parameters that describe the trapping effect. In particular: k is related to the hydrogen atoms captured per second and p is related to the probability that a trap containing a hydrogen atom will release it before 1 s is passed.

The parameters k and p are function of temperature according to Arrhenius relationships [40]: (eq. (11)) (eq. (12)).

$$k = k_0 \exp\left(-\frac{E_t}{RT} \right) \tag{11}$$

$$p = p_0 \exp\left(-\frac{E_d}{RT} \right) \tag{12}$$

Oriani reformulated this model by assuming that the hydrogen concentration in trap sites C_T depends only on the hydrogen concentration in lattice sites. Θ_L is the occupancy of lattice sites. N_L and N_T are the available sites. The equilibrium between the two population is described by the constant K: (eq. (13)).

$$K = \frac{1 - \theta_L}{\theta_L} \left(\frac{\theta_T}{1 - \theta_T} \right) \tag{13}$$

1.5. Hydrogen diffusion coefficients determination

Electrochemical techniques are used to determine the hydrogen diffusion coefficient for a material. During the electrochemical tests, metallic specimens are used as membranes to obtain the trend of the permeation of the specimen as a function of time.

The permeation of flux i_∞ can be defined as the diffusion of hydrogen across the membrane on the supposition that the entry of hydrogen into the steel surface is an intermediate adsorption-absorption reaction within local equilibrium reaction.

For this boundary condition, it is assumed that the amount of hydrogen in the specimens rises over time, leading to a corresponding rise in the permeation current density as measured at the exit surface, where zero hydrogen concentration is defined as hydrogen that has totally completed oxidation.

At steady state, the permeation transient reaches its maximum and the concentration profile of hydrogen permeation is relatively flat linear and does not change with permeation time. As a result, the hydrogen permeation or current density in the final state is given by eq. (14).

$$\Delta i_\infty = \frac{F D_L C_0}{d} \tag{14}$$

where D_L is the effective hydrogen diffusion coefficient, C_0 is the hydrogen subsurface concentration, and d is the membrane thickness, F is the Faraday's constant.

The hydrogen flux or permeation rate is directly related to the hydrogen subsurface concentration at the cathodic side, which has been experimentally determined in earlier contributions by using eq. (15). This is because there is a difference in hydrogen concentration between the entry surface and the exit surface of the specimen.

$$J = \frac{\Delta i_\infty}{F} = \frac{D_L C_0}{d} \tag{15}$$

where J represents the hydrogen flow across the steel specimen. Quantitative analysis can be used to assess hydrogen diffusion coefficients after permeation experiments have produced findings for the hydrogen transient curve dependent on time.

1. Inflection point method
2. Breakthrough time method
3. Time lag method

The crystal structure significantly influences atomic hydrogen transport in metallic materials [35,36,41,42], with hydrogen solubility being higher in fcc-crystals than in bcc-crystals. Hydrogen-induced distortions in unstrained lattices affect diffusivity, altering the local electronic structure of metal atoms and potentially decreasing interatomic cohesion, resulting in embrittlement [21]. Hydrogen oversaturation can lead to metal hydride formation, impacting austenitic steels. The hydrogen-enhanced decohesion (HEDE) theory suggests hydrogen in the lattice weakens atomic cohesion, contributing to cracking under tensile stresses, particularly in the crack tip [43,44].

Hydrogen embrittlement can also occur through the hydrogen Dislocation Interaction theory, affecting dislocation mobility and material fracture behavior. The Hydrogen Enhanced Localised Plasticity (HELP) mechanism integrates various research, proposing that hydrogen in solid solution increases dislocation mobility, causing localized plasticity deformation and lowering the critical stress for crack initiation. According to the theory of hydrogen vacancy interactions, hydrogen can generate Superabundant Vacancies (SAV), leading to microcrack or microvoid formation and decreasing material ductility [45,46].

Based on the presented literature review, we conclude that there are not yet too many works on 3D microstructure modeling that takes into account the substructures resulting from the structural elements of the austenitic stainless-steel microstructure. Therefore, the effects of structural parameters such as grain boundaries and dislocations have yet to be thoroughly investigated and discussed in detail. For this reason, this thesis aims to investigate the effects of microstructural features such as grain boundaries, precipitates and dislocations on hydrogen diffusion and embrittlement in order to gain a comprehensive understanding of how these factors influence the susceptibility of austenitic stainless steels to hydrogen embrittlement. In this paper, all these are analysed and an FEM model is implemented in Ansys capable of simulating the diffusion of hydrogen for a microstructure of austenitic stainless steel.

Using the theories of McNabb & Foster and Oriani, a model is implemented to simulates the interaction between hydrogen atoms and the lattice, understanding the effects of traps.

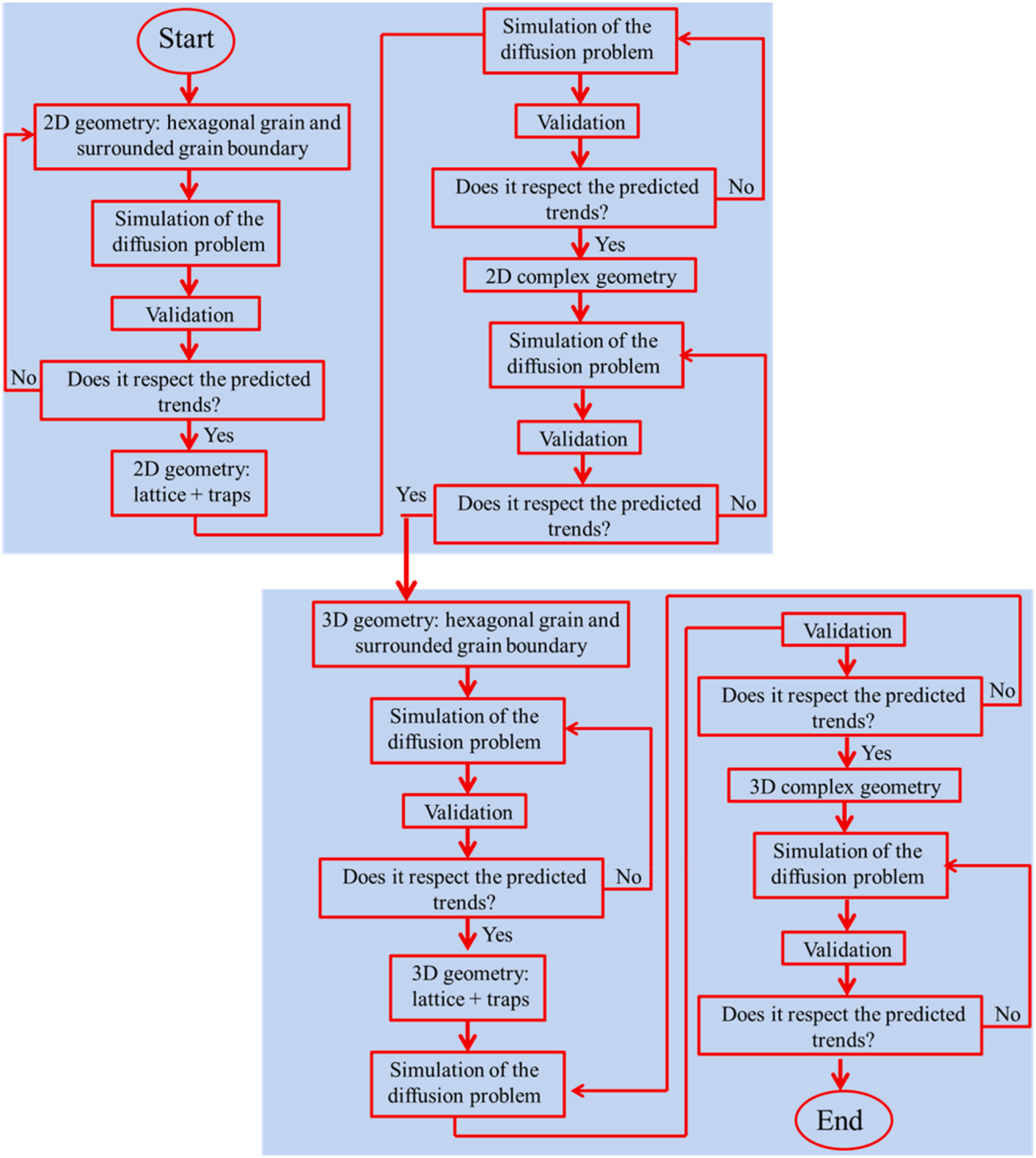

Fig. 1. Models implementation flowchart.

2. Model implementation

To implement the hydrogen transport equation, it's possible to use the similarities with the heat equation. This similarity allows to simulate the phenomenon of hydrogen diffusion in any FEM software in which this equation is implemented. In this work Ansys Workbench and Mechanical APDL are used.

The heat equation is represented by the following expression (eq. (16)):

$$\rho c_p \frac{\partial T}{\partial t} + \nabla \bullet \overline{J_q} + r_q = 0 \tag{16}$$

In the heat equation the degree of freedom is the temperature T, the temperature is substituted by the hydrogen concentration in lattice C_L. Density ρ and specific heat c_p in the heat equation are set equal to one in the hydrogen diffusion expression. By employing this manipulation, it becomes achievable to equate the material conductivity (k) with the hydrogen diffusion coefficient (D_L). r_q is the heat source that in the diffusion problem becomes hydrogen source rm and set equals to zero. J_q is the heat flux that in the diffusion equation becomes the hydrogen flux J.

The heat equation (eq. (17)): becomes:

$$1 * \frac{\partial C_L}{\partial t} + \nabla \bullet \overline{J} + r_m = 0 \tag{17}$$

In the models the heat equation is used two times to simulate the hydrogen diffusion in two different conditions.

The model was implemented by increasing the degree of complexity. The first model is a 2D pure diffusion problem in a microstructure formed by a single grain and his boundary grain (hexagon). After this

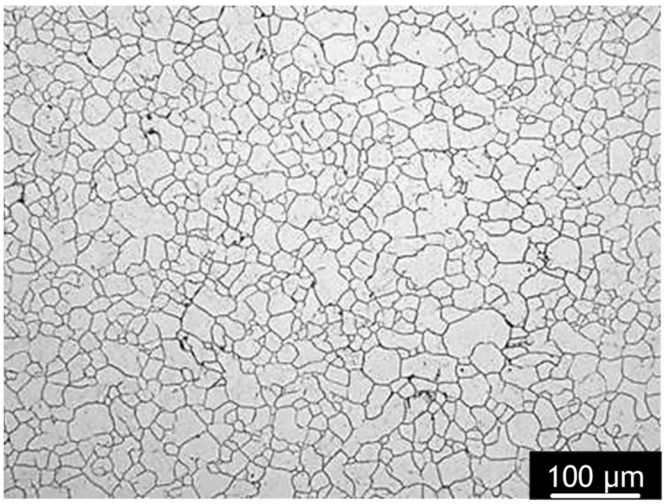

Fig. 2. Micrograph of the austenitic microstructure.

step, the traps such as dislocation, precipitates, and vacancies are implemented.

The second model is a 3D pure diffusion problem in a microstructure formed by a single grain and his boundary grain (icosahedron). After this step were implemented the traps such as dislocation, precipitates, and vacancies. Fig. 1 show the flowchart of the steps followed for the implementation of the model.

2.1. 2D models

The model is based on an austenitic stainless-steel microstructure whose primary crystalline structure is austenite. Fig. 2 shows a micrograph of the austenitic microstructure.

For the selected metal the average area of a single grain is 100 [um^2]. To make the model more efficient, a single grain was initially analysed and then a more complex geometry. The single grain has a hexagon shape whit an area of 100 [um^2].

The trend of diffusion coefficient of the austenitic lattice in function of the temperature is reported in Fig. 3 (a).

The traps that are simulated are of four types: boundary grains, dislocation, precipitates, and vacancies.

2.2. 2D boundary grains

Boundary grains have a high impact for the diffusion of hydrogen on metals. These traps are preferential phat for the diffusion of hydrogen. In general, the diffusion coefficient of boundary grain in greater than three

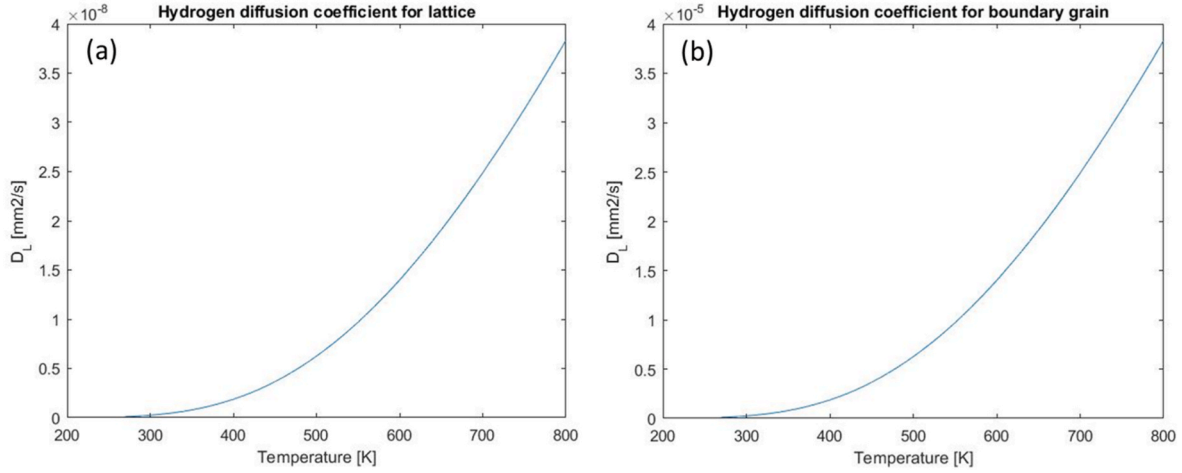

Fig. 3. Hydrogen diffusion coefficient of (a) the lattice, and (b) the boundary grain in function of the temperature.

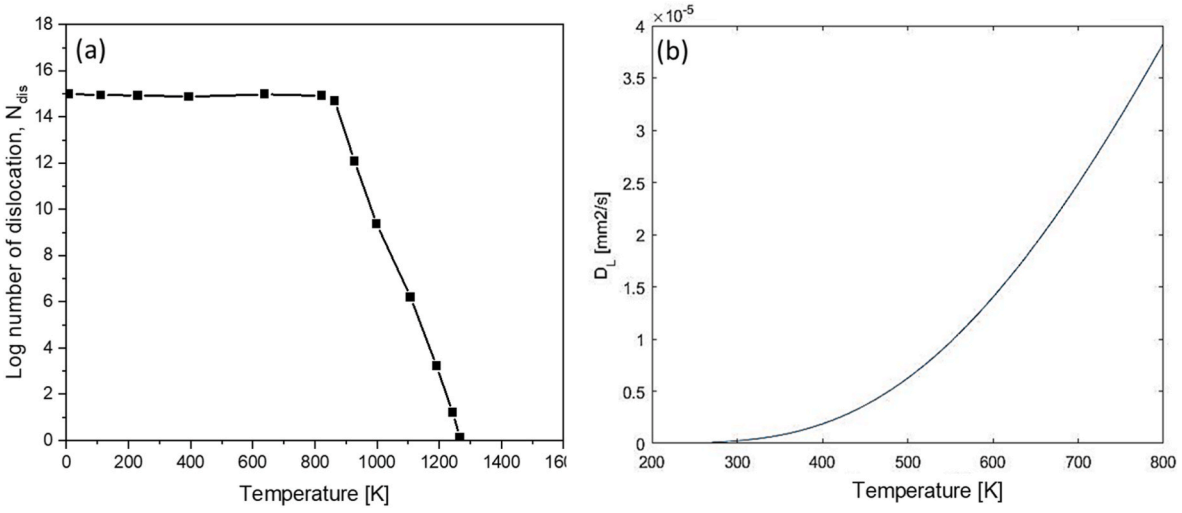

Fig. 4. (a) Number of dislocations in the lattice, (b) Hydrogen diffusion coefficient of the dislocations in function of the temperature.

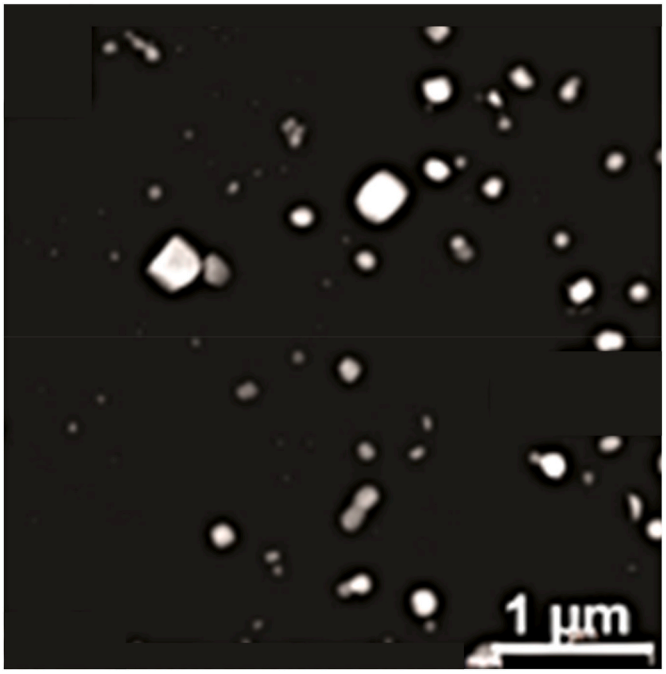

Fig. 5. EDX-spectral maps of carbide and nitro-carbide precipitates extracted from X20CrNiMnVN18-5-10.

Table 2
Summary of the results of the spectral analysis.

Type of precipitate	Average diameter [nm]	Number of precipitates in the reference area	Total area of precipitate in the reference area [um^2]	Normalized percentage of precipitate area
1	323,5	2	164 304,0325	0,89 %
2A	147,1	25	424 653,7963	2,30 %
2B	97,1	29	214 637,7537	1,16 %
3	38,3	49	56 423,92 385	0,31 %

orders of magnitude than lattice. Boundary grain material is implemented to simulate the effect of the boundary grain. This material has the same mechanical properties of the lattice, but it has different diffusion coefficient. The boundary grains diffusion coefficient is function of the temperature.

The expression (eq. (18)) of the diffusion coefficient for the grain boundary is:

$$D_{L_{GB}} = D_{L_{0_{GB}}} * \exp\left(-\frac{E_L}{RT}\right) \tag{18}$$

The trend of this coefficient in function of the temperature is shown in Fig. 3 (b). The dimension and the number of the boundary grains are constant for all the temperature.

2.3. 2D dislocations

Dislocations are simulated as saturable traps. The number and the diffusive properties of the dislocations are function of the temperature.

Austenitic stainless steel subjected to the extrusion process has a dislocation density equal to 10^{16} $\left[\frac{dislocation}{m^2}\right]$. The number of dislocations is function of temperature is constant for temperature lower than 600 °C. For temperature greater than 600 °C dislocation's number has a linear decreasing trend up to 10^{12} $\left[\frac{dislocation}{m^2}\right]$ for temperature equal to 1000 °C.

Fig. 4(a) represents the trend of the dislocations number in function of the temperature.

A specific material is implemented to simulate the effect of the dislocations in the diffusion path. This material has the same mechanical properties of the lattice, but it has a different diffusion coefficient. The diffusion coefficient is function of temperature. The quantity of hydrogen that saturates the dislocation is set equal to the quantity that saturates the lattice. To explain why the number of dislocations in the lattice is constant up to $\sim 900\ ^{\circ}C$, the presence of hydrogen in the lattice should be considered. Hydrogen in the lattice acts as a conventional means of strengthening the solid solution and hinders the movement of the dislocations [2]. The entrainment of the hydrogen atmosphere with the dislocations provides a natural explanation for the limitation of transverse slip and the increase in slip flatness, since the hydrogen atmosphere would have to be redistributed to allow the constriction or for the dislocation to reorient itself into the necessary screw configuration. There is no additional driving force that could accomplish this, and consequently the dislocations are forced to continue sliding on the

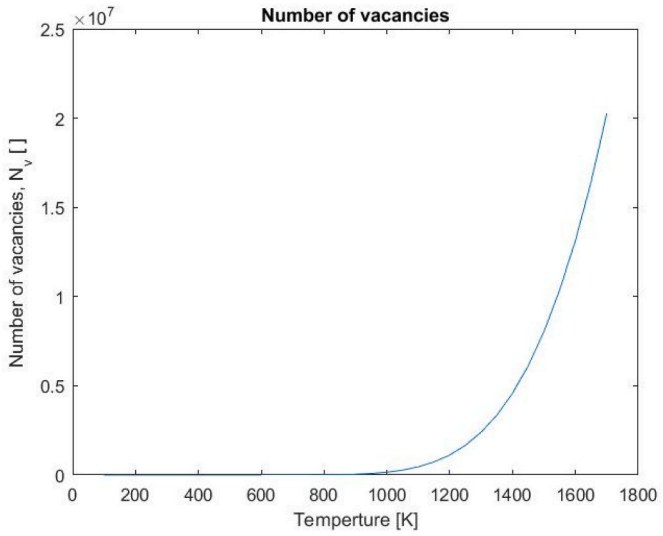

Fig. 6. Number of vacancies if function of the temperature.

Table 3
Summarized results for precipitates calculations.

Type of precipitate	Crystal structure	Lattice parameter: a [Å]	Lattice parameter: b [Å]
1	Cubic	3,4	–
2A	Orthorhombic	11.47	5.54
2B	Orthorhombic	5.07	4.51
3	Cubic	4,15	–
Type of precipitate	**Volume available for hydrogen atoms [pm^3]**	**Area available for hydrogen atoms [pm^2]**	**Value of max saturation respect to grain boundary**
G1	$1.7 * 10^7$	$1.2 * 10^5$	70 %
G2A	$1.07 * 10^8$	$3.3 * 10^5$	60 %
G2B	$6.2 * 10^7$	$2.9 * 10^5$	60 %
G3	$2.1 * 10^7$	$2.1 * 10^4$	50 %

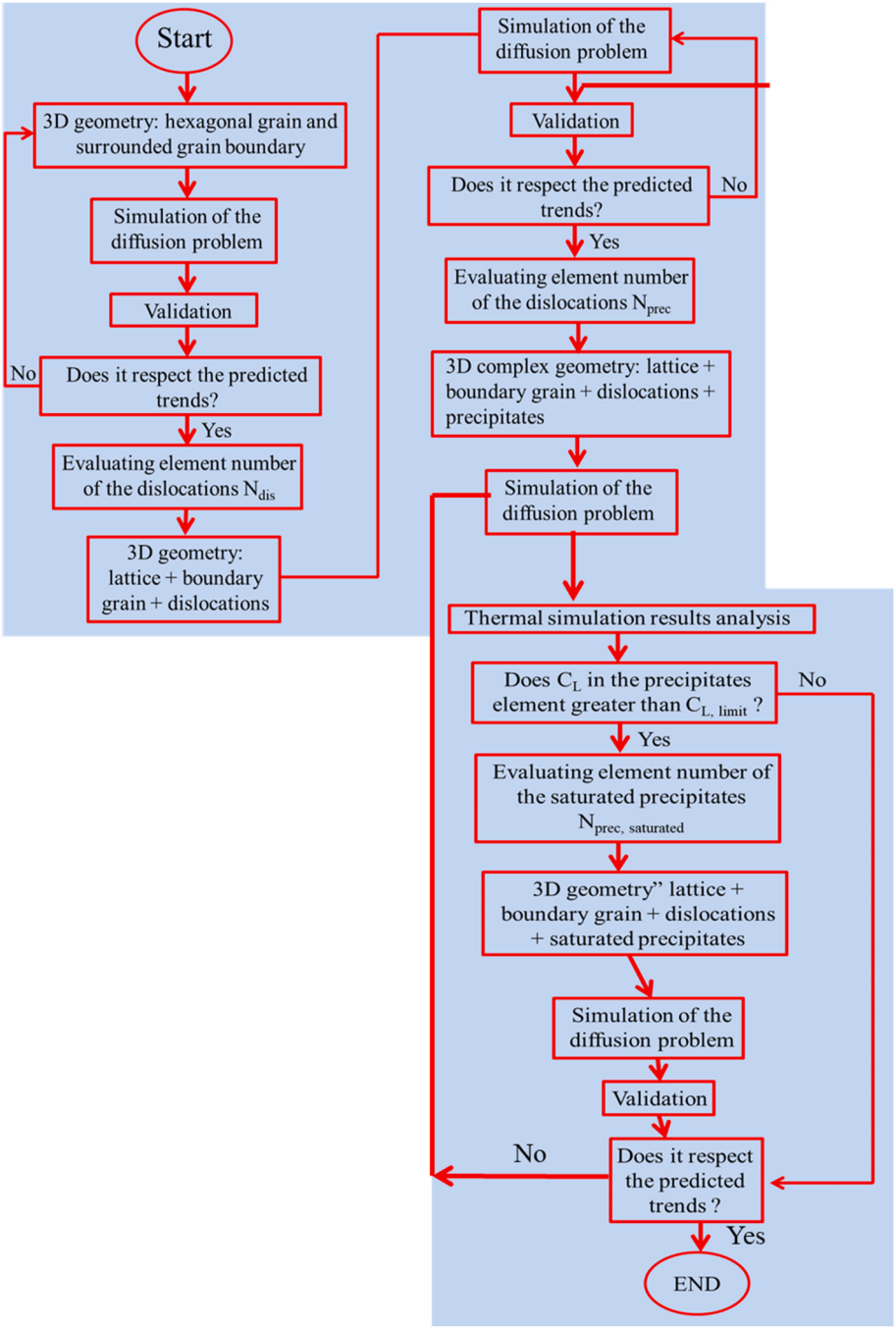

Fig. 7. 3D model implementation flowchart.

Table 4
3D model design parameters.

Design parameter	Value
Grain volume [um^3]	185,44
Boundary grain thickness [um]	1,5
Boundary grain volume [um^3]	102,68
Total volume [um^3]	288,12

primary slip plane. This locking of the dislocations to a particular slip plane, which prevents lateral sliding, has been observed experimentally [47,48].

Fig. 4(b) shows the trend of the dislocation diffusion coefficient in function of the temperature.

Precipitates are modelled as irreversible traps. Four types of precipitates are considered which correspond to different size and composition of the precipitates: The first type (>200 *nm*) that comprises Vanadium carbides and Vanadium nitrides, Type 2A and 2B (=100 *nm*) that comprises Chromium carbides and Iron carbides and type 3 (=20 *nm*) that comprises Chromium nitrides.

The analysis of thermal desorption spectroscopy (TDS) performed on stainless steel has demonstrated that hydrogen diffusion path is highly influenced by the number of precipitates and their size.

Fig. 5 shows EDX-spectral maps of carbide and nitro-carbide precipitates extracted from. From Fig. 7 it's possible to notated that there are four types of precipitates. The size of the area where the analyzes were performed is 18.5 [um^2].

Table 2 summarized the results of the spectral analysis performed on